

ESD RECORD COPY

RETURN TO
SCIENTIFIC & TECHNICAL INFORMATION DIVISION
(ESTI), BUILDING 1211

129

COPY NR. _____ OF _____ COPIES

RESULTS OF DETAILED FLOW FIELD AND RATE CHEMISTRY CALCULATIONS
ON AN AEROBALLISTIC PELLET

GASL Report TR-292

ESTI PROCESSED☐ DDC TAB ☐ PROJ OFFICER☐ ACCESSION MASTER FILE☐ _____

by

Arthur Fields

DATE _____

ESTI CONTROL NR. AL-40801CY NR. 1 OF 1 CYS

June 1962

Reissued September 18, 1962

The work reported in this document was performed at General Applied Science Laboratory, Inc. for M. I. T. Lincoln Laboratory under Subcontract No. 226; this work was supported by the U.S. Advanced Research Projects Agency under Air Force Contract AF 19(604)-7400 (ARPA Order 13).

When US Government drawings, specifications or other data are used for any purpose other than a definitely related government procurement operation, the government thereby incurs no responsibility nor any obligation whatsoever; and the fact that the government may have formulated, furnished, or in any way supplied the said drawings, specifications, or other data is not to be regarded by implication or otherwise as in any manner licensing the holder or any other person or conveying any rights or permission to manufacture, use, or sell any patented invention that may in any way be related thereto.

Qualified requesters may obtain copies from Defense Documentation Center (DDC). Orders will be expedited if placed through the librarian or other person designated to request documents from DDC.

Copies available at Office of Technical Services, Department of Commerce.

Do not return this copy. Retain or destroy.

Publication of this technical documentary report does not constitute Air Force approval of the report's findings or conclusions. It is published only for the exchange and stimulation of ideas.

TECHNICAL REPORT No. 292

RESULTS OF DETAILED FLOW FIELD
AND RATE CHEMISTRY CALCULATIONS
ON AN AEROBALLISTIC PELLET

By Arthur Fields

SUBCONTRACT NO. 226

Prepared For

Massachusetts Institute of Technology
Lincoln Laboratory
Lexington 73, Massachusetts

Prepared By

General Applied Science Laboratories, Inc.
Merrick and Stewart Avenues
Westbury, L.I., New York

June, 1962

Approved by: _____



Antonio Ferri
President

TABLE OF CONTENTS

<u>Section</u>	<u>Title</u>	<u>Page</u>
	List of Figures	iii
I	Introduction	1
II	Discussion of Results	3
III	Summary	9
	References	10
	Table I	4
	Figures 1 through 15	11

LIST OF FIGURES

<u>Figure Number</u>	<u>Title</u>	<u>Page</u>
1	Aeroballistic Pellet Geometry	11
2	Flow Field Details	12
3	Electron Density Distribution Along the Body Streamline, $\theta_1 = 0.93046$ radians	13
4	Electron Density Distribution Along Streamline A $\epsilon = 1.1838$ radians	14
5	Electron Density Distribution Along Streamline B, $\epsilon = 1.0691$ radians	15
6	Electron Density Distribution Along Streamline C, $\epsilon = 1.0056$ radians	16
7	Electron Density Distribution Along Streamline D, $\epsilon = 0.81319$ radians	17
8a	Electron Density Distribution Along Streamline E, $\epsilon = 0.51777$ radians, Initial Species Concentration Behind the Bow Shock Taken at the Equilibrium Dissociation Values	18
8b	Electron Density Distribution Along Streamline E (cont'd), $\epsilon = 0.51777$ radians, Initial Species Concentration Behind the Bow Shock Taken at the Free Stream Values	19
9	Electron Density Distribution Across the Shock Layer, $S_{\text{body}} = .14506$	20
10	Electron Density Distribution Across the Shock Layer, $S_{\text{body}} = .55118$	21
11	Electron Density Distribution Across the Shock Layer, $S_{\text{body}} = .95729$	22

LIST OF FIGURES
(continued)

<u>Figure Number</u>	<u>Title</u>	<u>Page</u>
12	Electron Density Distribution Along Axis of Far Wake	23
13	Temperature Distribution Along Axis of Far Wake	24
14	Density Distribution Along Axis of Far Wake	25
15	Velocity Distribution Along Axis of Far Wake	26

RESULTS OF DETAILED FLOW FIELD
AND RATE CHEMISTRY CALCULATIONS
ON AN AEROBALLISTIC PELLET

By Arthur Fields

I. INTRODUCTION

The method of characteristics as applied to a real gas (assuming frozen composition along streamlines) was used to compute the detailed supersonic flow field about the pellet geometry shown in Figure 1. The free stream velocity was 22,100 feet per second while the free stream pressure and temperature were 1 mm Hg and 300°K respectively.

The calculation of the flow field properties in the subsonic region was performed by applying the technique given in Reference 1 to a real gas. The air was assumed to be in thermal and chemical equilibrium. The results of this calculation served as input to the frozen characteristics program which handles the computation of the entire supersonic flow field region up to the near wake shock. Details of this frozen characteristics program may be found in Reference 2.

While both the subsonic and supersonic analyses have been programmed for the IBM 704 computer and are completely automatic, the calculation of the wake shock was carried out by use of a Bendix G-15 computer. This calculation requires monitoring because of the limited storage capacity of the computer. The flow field downstream of the

Summary
on page 10
Type out
the info
in item 1
W

wake shock is calculated by the method of characteristics utilizing the IBM 704.

Thus, having completed the calculation of the detailed flow field about the pellet, we then proceeded to study the effects of rate chemistry. Because of the complexity of solving for the general flow field properties of a gas in non-equilibrium molecular dissociation, a one dimensional approach to the solution of this problem was used, (Reference 4.)

The solution of the detailed frozen flow field enables us to pick various streamlines in the flow field for the purpose of determining the effect of rate chemistry upon electron density. Prescribed pressure distributions along each streamline were given as inputs to this one dimensional calculation, the insensitivity of the rate processes to pressure distribution having been established in Reference 3. The gas was assumed to consist of a basic mass fraction composition of 0.234 oxygen, 0.766 nitrogen and to dissociate into a mixture involving seven chemical species, namely; N , N_2 , O , O_2 , NO , NO^+ , e^- , which partake in the following reactions:



Each individual component behaves as a thermally perfect gas, individually in thermal equilibrium, although it may partake in dissociative reactions. The details of this analysis may be found in Reference 4.

This non-equilibrium molecular dissociation calculation for the body streamline was continued to approximately 30 nose radii downstream where the pressure nearly approached the free stream value. The results served as input to the far wake analysis which is briefly discussed below.

The far wake analysis was carried out by utilizing the methods given in Reference 5 which involves an integral approach for the solution of the properties of a laminar, axisymmetric, hypersonic wake with coupled diffusion and rate chemistry. This integral technique involves the solution of the applicable conservation equations (mass, momentum, energy, and species) on the average over a normal cross-section, and exactly on the axis.

A discussion of the results of the preceding analyses may be found in the next section.

II. DISCUSSION OF RESULTS

The body streamline and five external streamlines were chosen to illustrate the effects of rate chemistry. The relative location and non-dimensional distance along each streamline may be found in Figure 2.

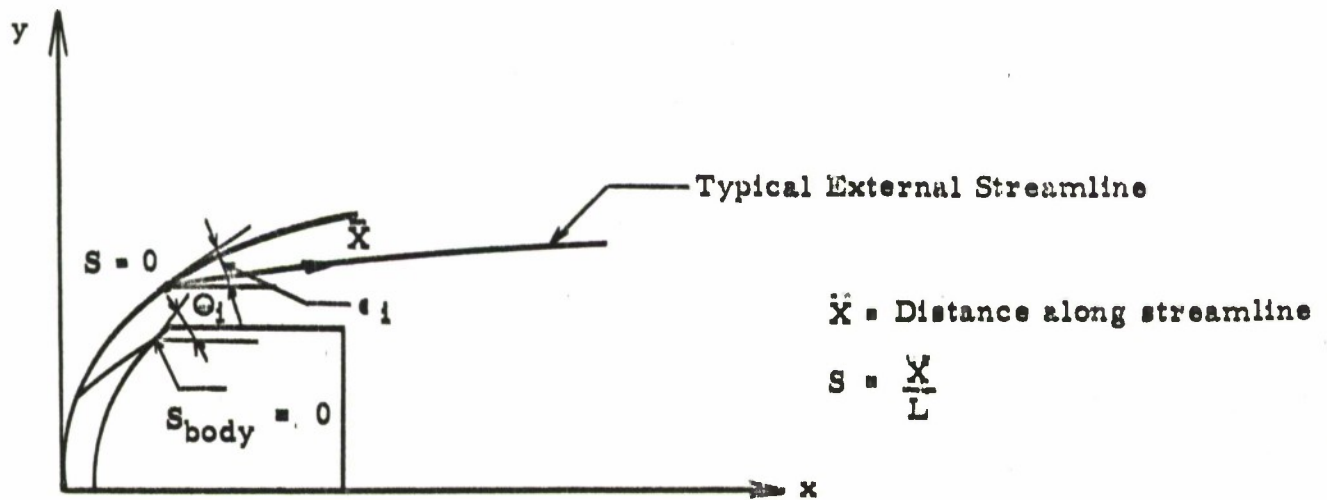
Table I below lists the shock inclination and entropy for each streamline.

The geometry is explained in Sketch 1.

Table I

Streamline Properties

Streamline	ϵ_1 , rads	Entropy, S/R	
		<u>Upstream of</u> <u>Wake Shock</u>	<u>Downstream</u> <u>of Wake Shock</u>
Body	$\theta_1 = .93046$	47.490	47.856
A	1.1838	46.652	47.043
B	1.0691	45.000	45.364
C	1.0056	44.348	44.636
D	.81319	41.793	41.796
E	.51777	37.690	---



Sketch 1

Figure 3 shows the electron density distribution along the pellet body streamline, where the initial specie mass fractions were taken at their equilibrium dissociation values. No comparison was made with a flow model which assumes that the initial species concentration is equal to the free stream composition since previous studies have shown the flow along the body streamline to be in local equilibrium up to the vicinity of the sonic line. The isolated points indicate the local equilibrium values, i. e., the electron density which would exist if the ionization were in equilibrium with the local frozen concentrations of atomic oxygen and nitrogen. Note that for small values of S , the electron density is close to the local equilibrium value, but the expansion corner causes considerable deviation which persists along the remainder of the body streamline. The second discontinuity in electron density occurs at the base of the pellet where the flow expands to the base pressure. The third discontinuity represents the pressure jump which occurs at the beginning of the wake shock.

Figures 4, 5, 6, 7 and 8, give the electron density distribution resulting from the rate chemistry calculations along external streamlines in the flow field. Initial points for the non-equilibrium dissociation calculation and the relative position of each streamline may be found in Figure 2. The dashed curve represents the electron density distribution resulting from the initial species concentration taken at its equilibrium dissociation

value. The solid curve shows the distribution resulting from the initial species concentration taken equal to the free stream value ($\alpha_{O_2} = .234$, $\alpha_{N_2} = .766$). Note that for streamlines A and B (Figures 4 and 5) the electron density distribution given by the initial frozen free stream composition assumption rapidly approaches local equilibrium, and in fact for Streamline A overshoots, and then closely follows the distribution given by the equilibrium dissociation assumption, although neither distribution can maintain the local equilibrium value for non-dimensional distances greater than $S = 0.2$.

Quite a different situation exists for streamlines D and E, (Figures 7 and 8). Here the distribution corresponding to initial free stream composition does not approach local equilibrium and is several orders of magnitude apart from the curve giving the electron density resulting from the equilibrium dissociation assumption.

The results of the nonequilibrium calculation for streamline C represents a borderline case. For small S the electron density distribution does not attain local equilibrium although it closely approaches it and beyond $S = 0.4$ both distributions do not differ by more than a factor of 3.

In summary then, the results of the rate chemistry calculations point to the existence of two regions in the flow field even for the small body geometry considered here. The first region is characterized by relaxation distances which are small when compared to the nose radius and includes the streamlines crossing a strong bow shock. The flow in the second region is characterized by large streamwise pressure variations over the relaxation distance. The flow entrained within the first region approaches local equilibrium and atomic recombination freezes while the recombination of ions and electrons persists due to its faster rate. Within the second region the flow never attains local equilibrium, the peak values of dissociation and ionization being realized before the onset of freeze due to the interaction between the driving conditions for dissociation and the damping effect of the rapid streamwise pressure/temperature decay.

Figures 9, 10, and 11 give the electron density profiles in the shock layer at the 1st expansion corner, midway back on the pellet ($S = 0.55118$) and at the pellet base, respectively. These figures illustrate the normal variations in electron density which exist due to rate chemistry considerations.

Figures 12, 13, 14, and 15 show the axial distribution of electrons, temperature, density and velocity in the far wake respectively. The solid curve represents the results of the present detailed analysis; the dashed curve taken from Reference 6 and included for comparison, shows the results of the approximate analysis. While differences in temperature, density and

velocity exist due to pressure differences, there is remarkably good agreement (Figure 12) in the electron density distribution which corroborates the approximate analysis scheme.

Results of the detailed rate chemistry analysis of the flow along streamlines in the shock layer and near wake flows indicates that due to the small size of the pellet the flow is essentially frozen down to the point where the far wake begins. Therefore since the wake input conditions are determined by the body streamline rate chemistry one should expect only minor differences between the initial conditions for the far wake calculations. In the far wake, as discussed in Ref. 6, due to the small dimensions involved, diffusion effects overwhelm the effects of rate chemistry to such an extent that the peaks in electron density predicted for a much larger vehicle and for which results are presented in Reference 7 are not observed.

III. SUMMARY

The detailed supersonic flow field about an MIT firing range pellet was computed by the method of characteristics. The a priori assumption of frozen air composition was made in light of the results given in Reference 3. This characteristics solution yielded pressure distributions which were used as input to a non-equilibrium molecular dissociation analysis along the body streamline and several other external streamlines in the flow field.

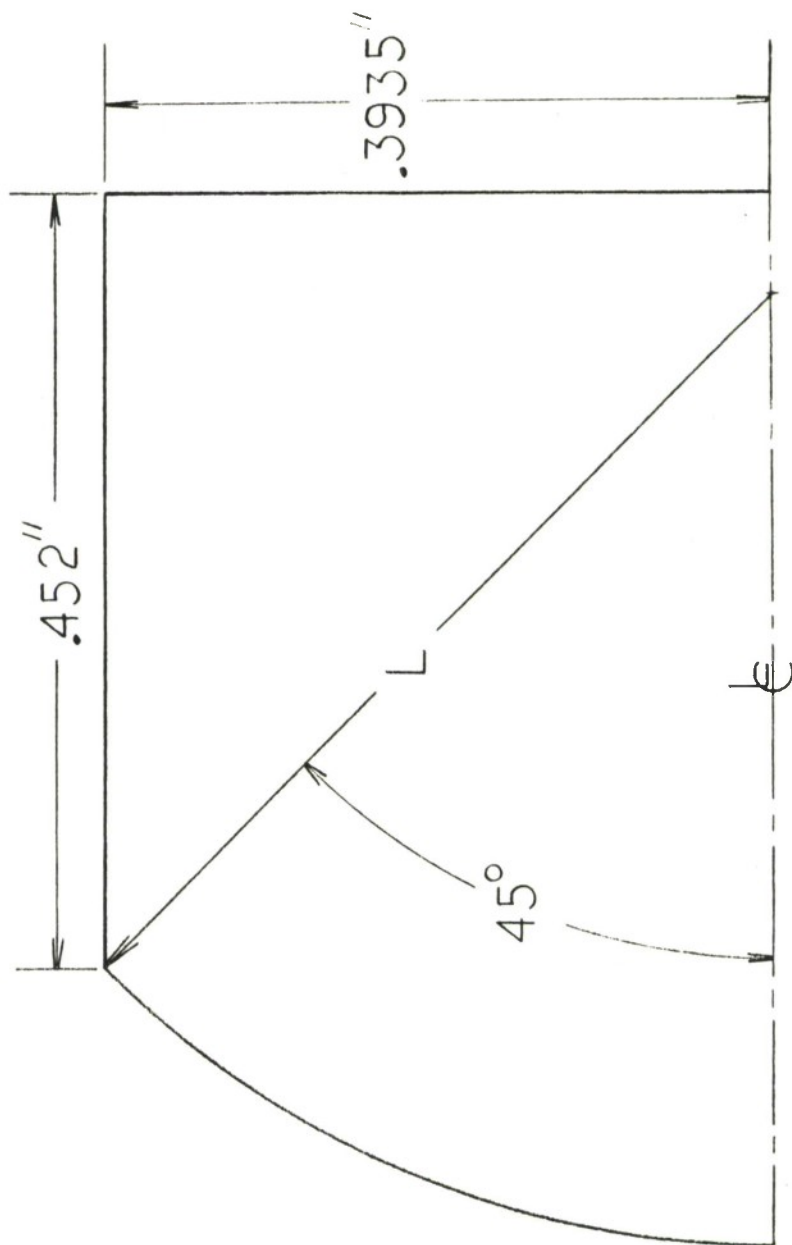
The effect of various flow model assumptions on electron density along each streamline is presented and electron density profiles across the shock layer are given for three axial stations.

The far wake analysis of Reference 5 was used to determine the axial electron density distribution a few hundred nose radii downstream of the pellet, and a comparison of the results thus obtained was made with those given by the approximate calculation of Reference 6. The agreement between the results of the actual and approximate calculations is excellent.

REFERENCES

1. Vaglio-Laurin, R. and Ferri, A., Theoretical Investigation of the Flow Field About Blunt-Nosed Bodies in Supersonic Flight. Journal of the Aerospace Sciences, Vol. 25, No. 12, pp. 761-770, December, 1958.
2. Lieberman, E. Description of IBM 704 Computer Programs For Calculation of Supersonic Flow Field Properties Using Frozen Chemistry. General Applied Science Laboratories, Inc., Technical Memo No. 62, April 1962.
3. Vaglio-Laurin, R., and Bloom, M. H., Chemical Effects in External Hypersonic Flows. International Hypersonics Conference Preprint Number 1976-61, August, 1961.
4. Steiger, M. H., Improved Rate Chemistry Program for One-Dimensional Inviscid Air Flow With Prescribed Pressure Variations. General Applied Science Laboratories, Inc. Technical Report No. 246, August 1961.
5. Steiger, M. H., Improved Hypersonic Laminar Wake Calculations Including Rate Chemistry. General Applied Science Laboratories, Inc. Technical Report No. 249, August, 1961.
6. Wecker, M. S., The Wake of An Aeroballistic Pellet, General Applied Science Laboratories, Inc., Technical Memo No. 61, March, 1962.
7. Bloom, M. H., Byrne, R. W., and Kennedy, E. D., Estimated Properties of Laminar Wakes with Coupled Rate Chemistry and Diffusion. General Applied Science Laboratories, Inc., Technical Report No. 282, May 1962.

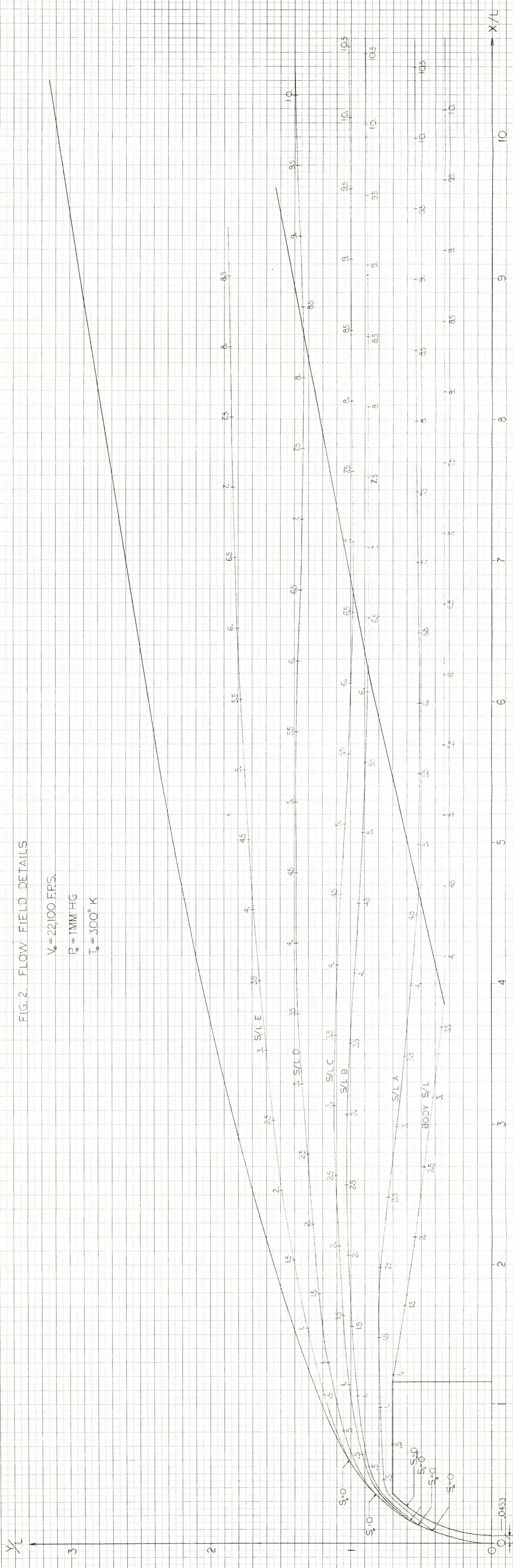
Fig. 1. Aeroballistic Pellet Geometry



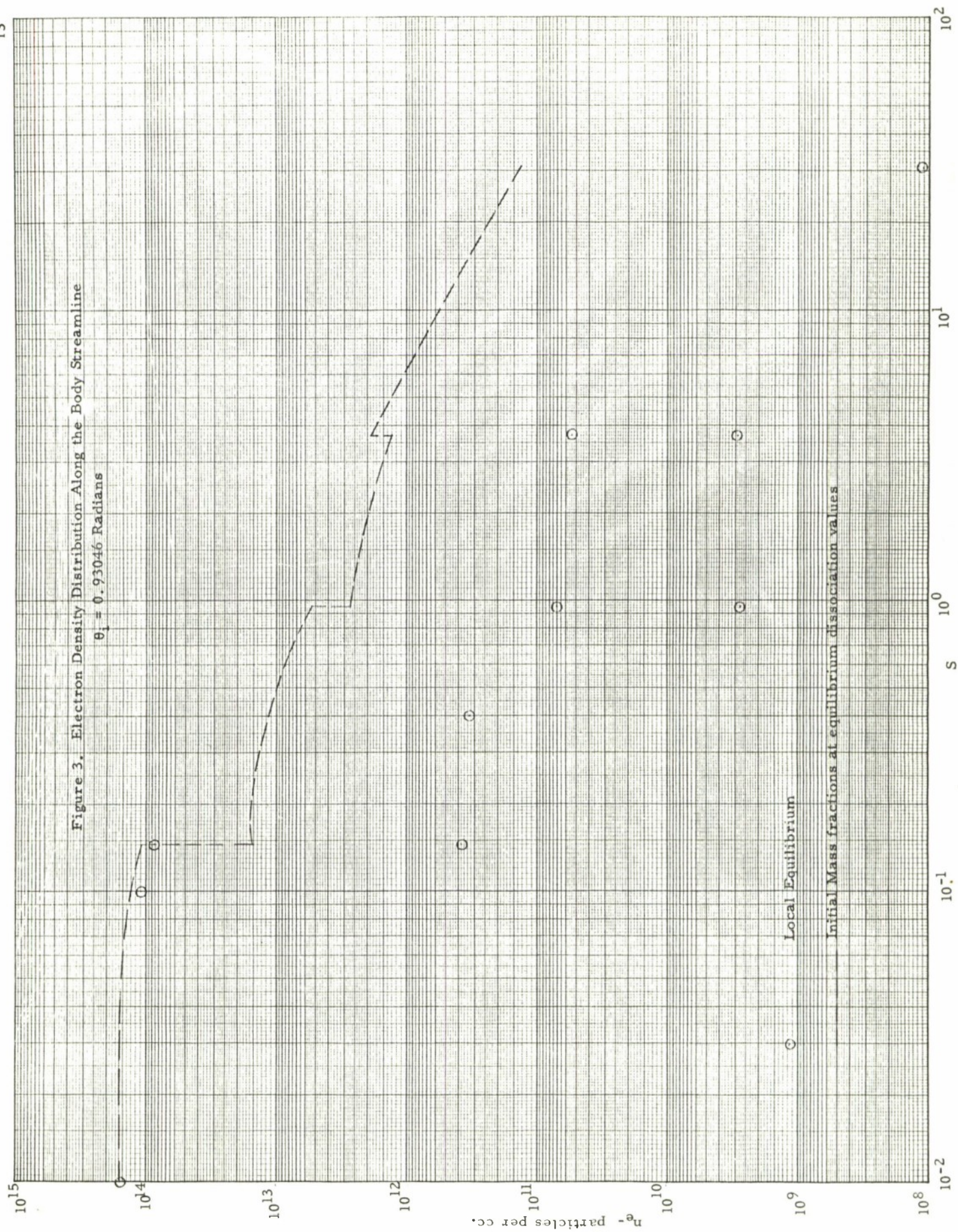
y/L

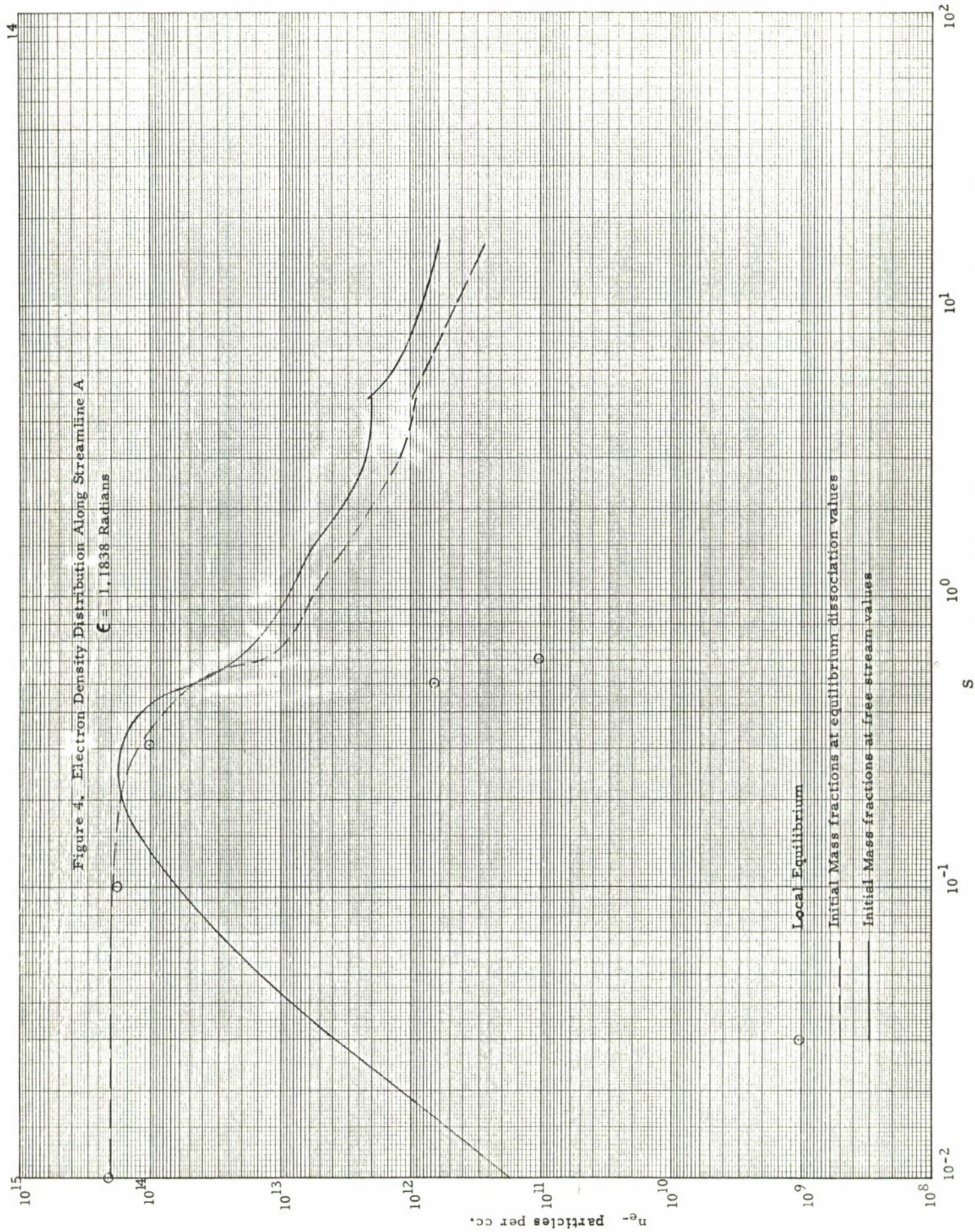
FIG. 2. FLOW FIELD DETAILS

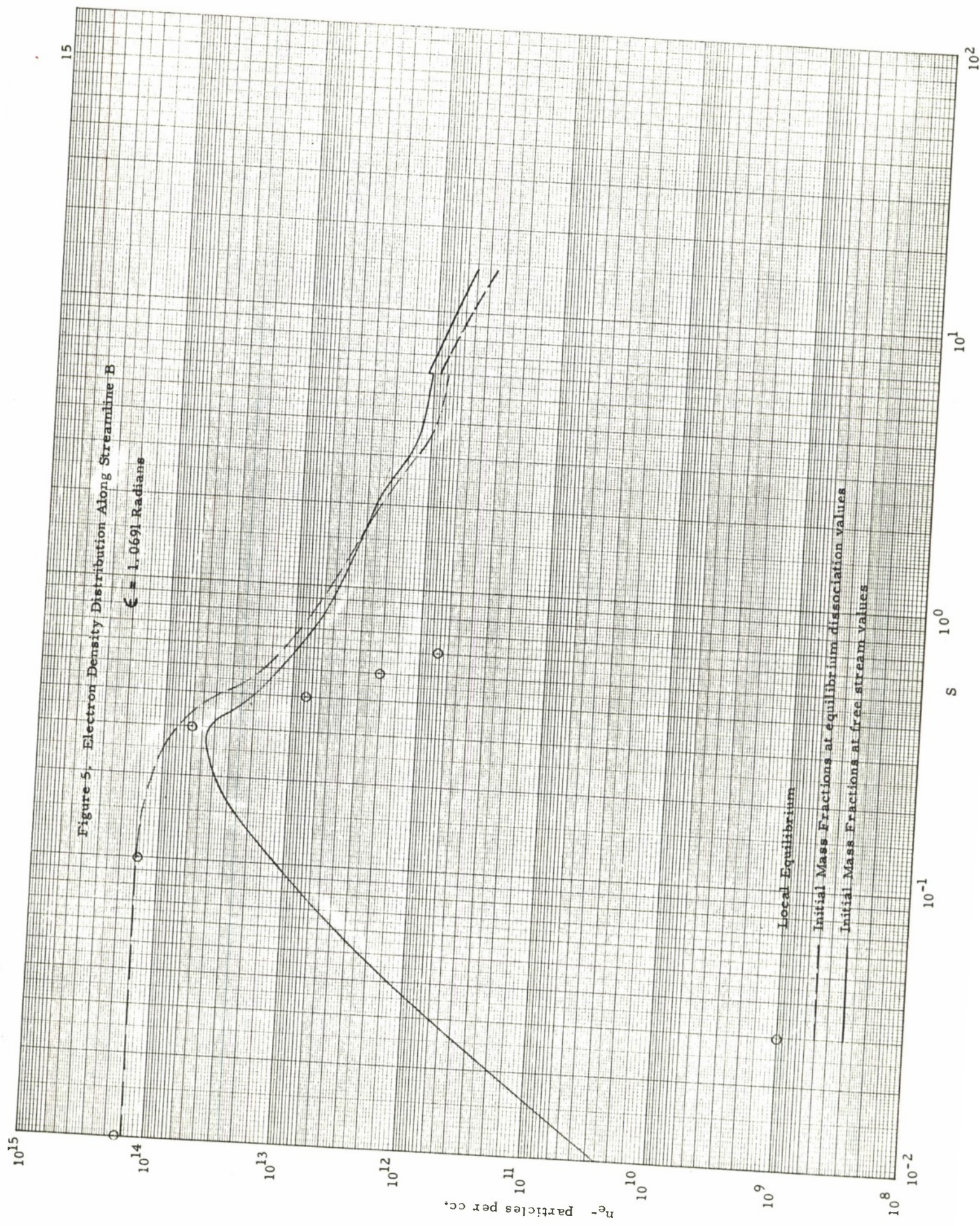
$V_\infty = 22,100$ FPS.
 $P_\infty = 1$ MM HG
 $T_\infty = 300^\circ$ K



x/L







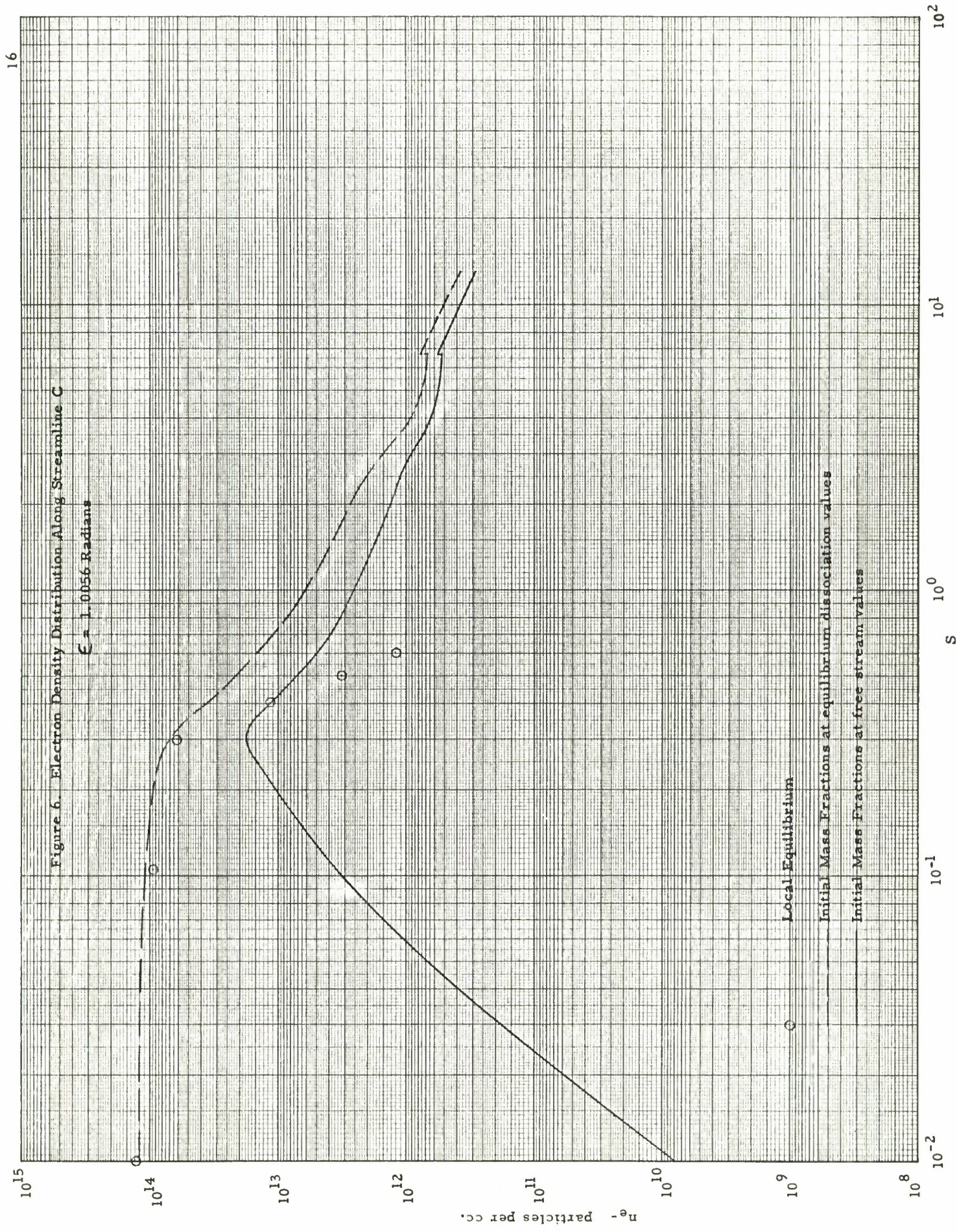
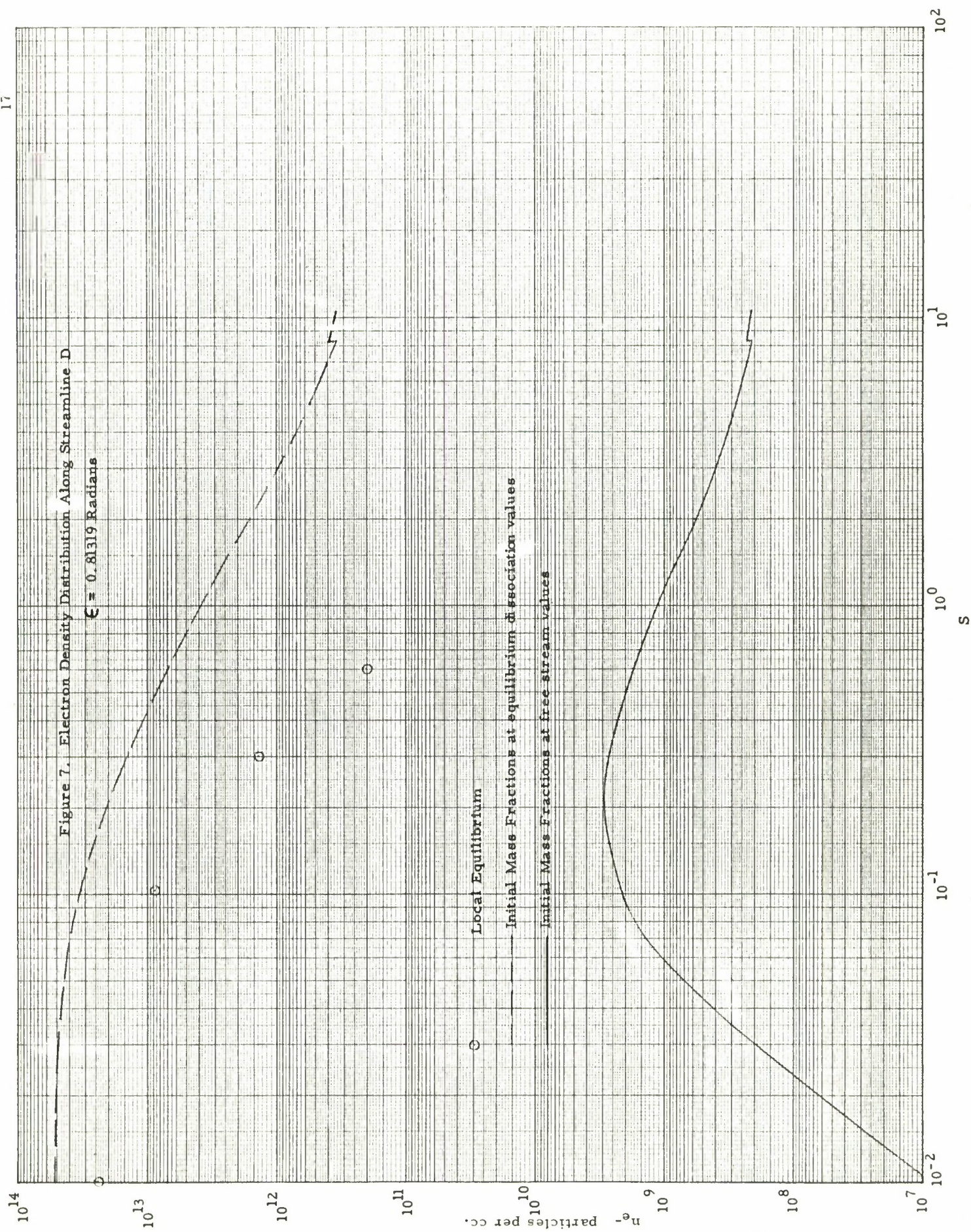
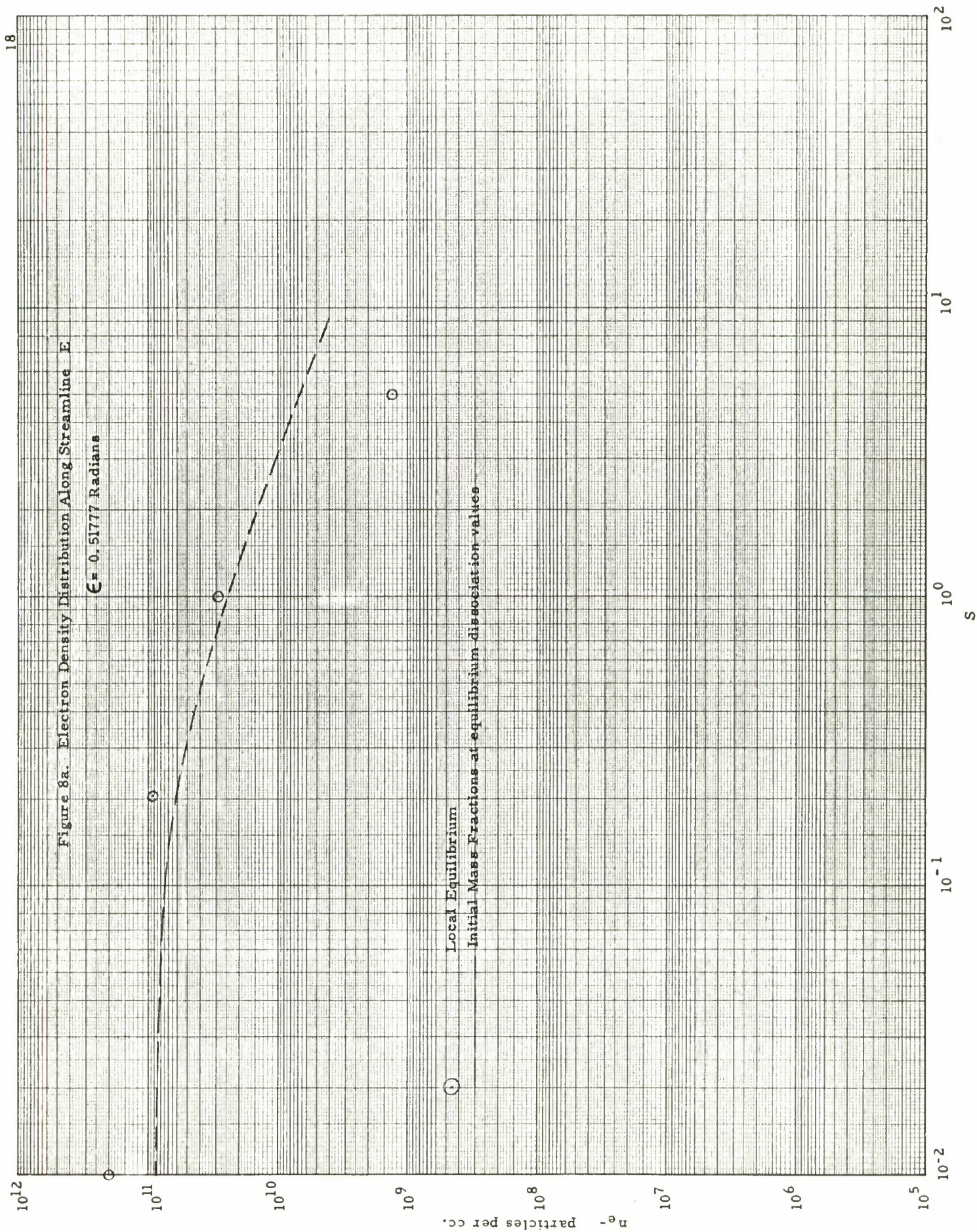
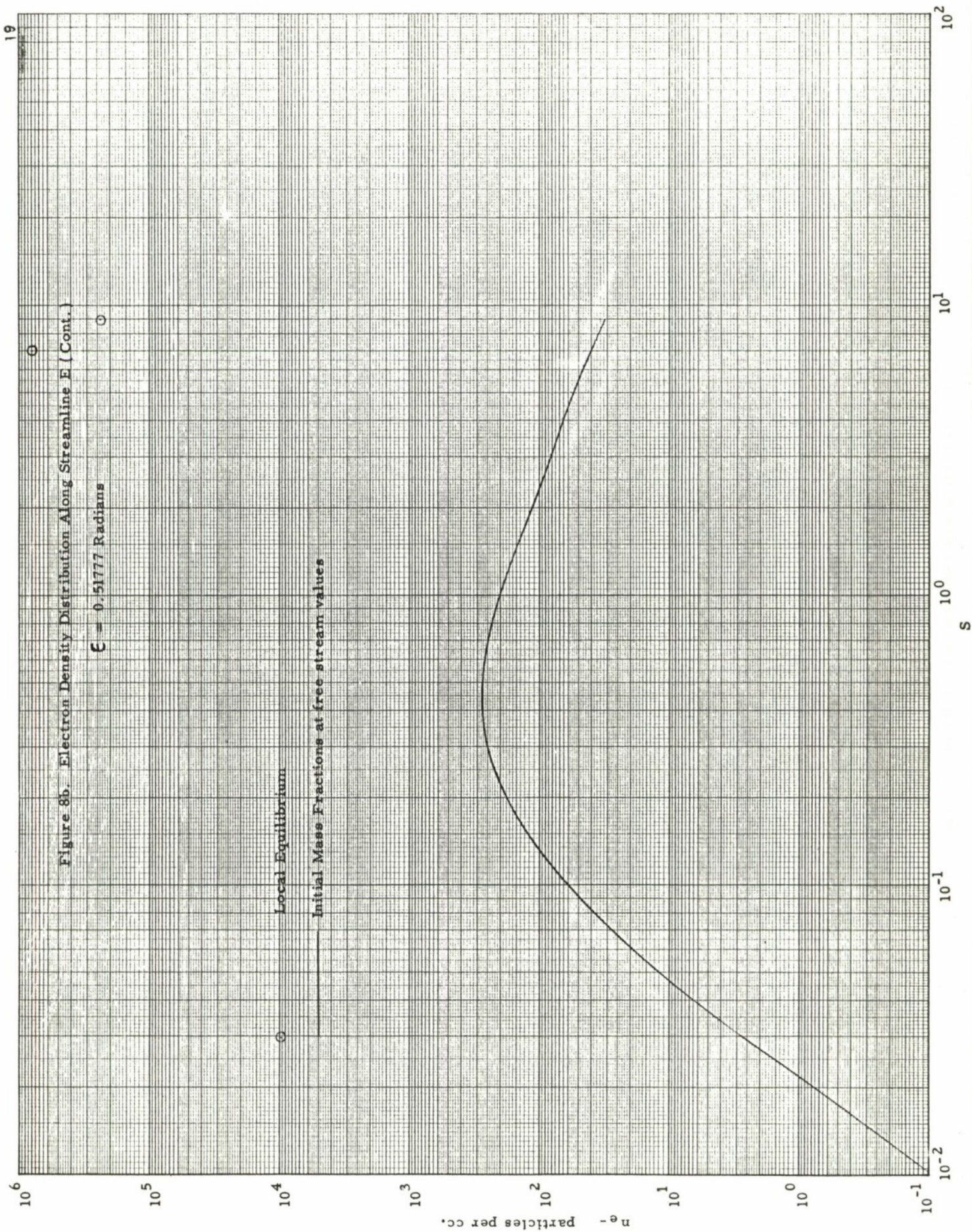


Figure 7. Electron Density Distribution Along Streamline D

 $\xi = 0.8319$ Radians





10¹⁵

20

Figure 9: Electron Density Distribution Across the Shock Layer

$$S_{\text{body}} = 0.14506$$

$$\bar{y} = \frac{y - y_{\text{body}}}{y_{\text{shock}} - y_{\text{body}}}$$

10¹⁴

$$y_{\text{body}} = 0.7071L$$

$$y_{\text{shock}} = 0.83L$$

10¹³

Initial Mass Fractions at Equilibrium Dissociation Values

Initial Mass Fractions at Free Stream Values

10¹²

0

.2

.4

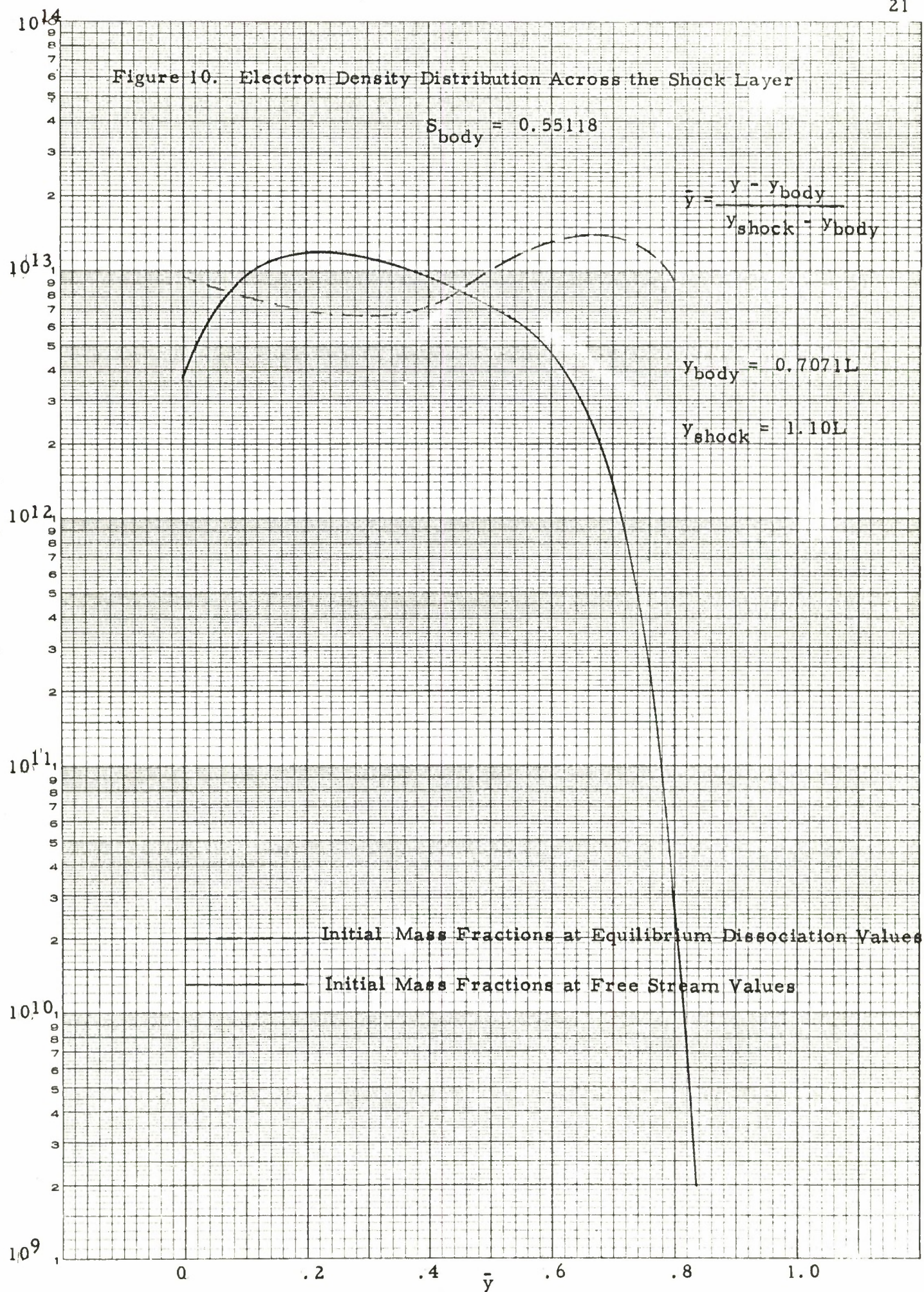
\bar{y}

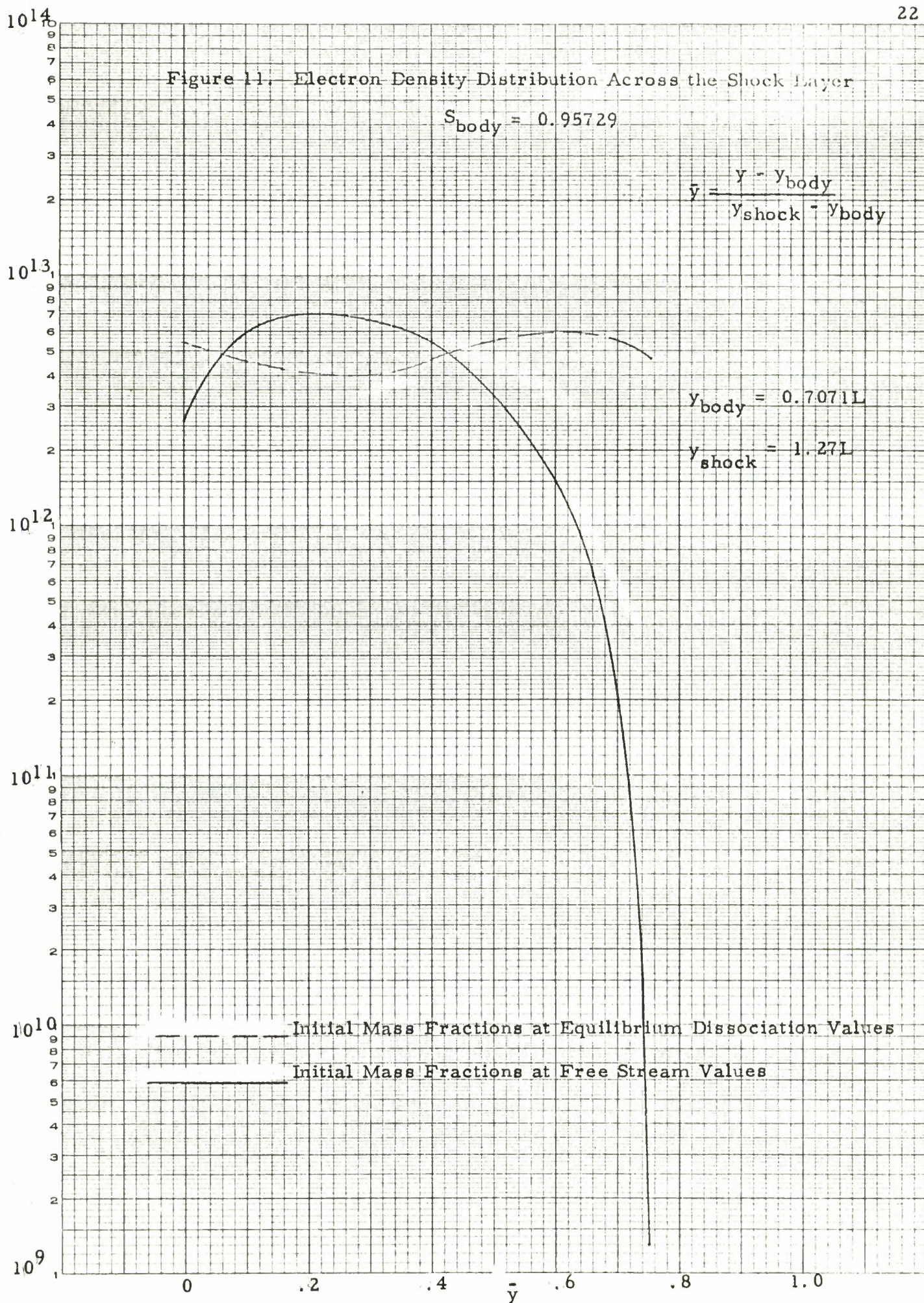
.6

.8

1.0







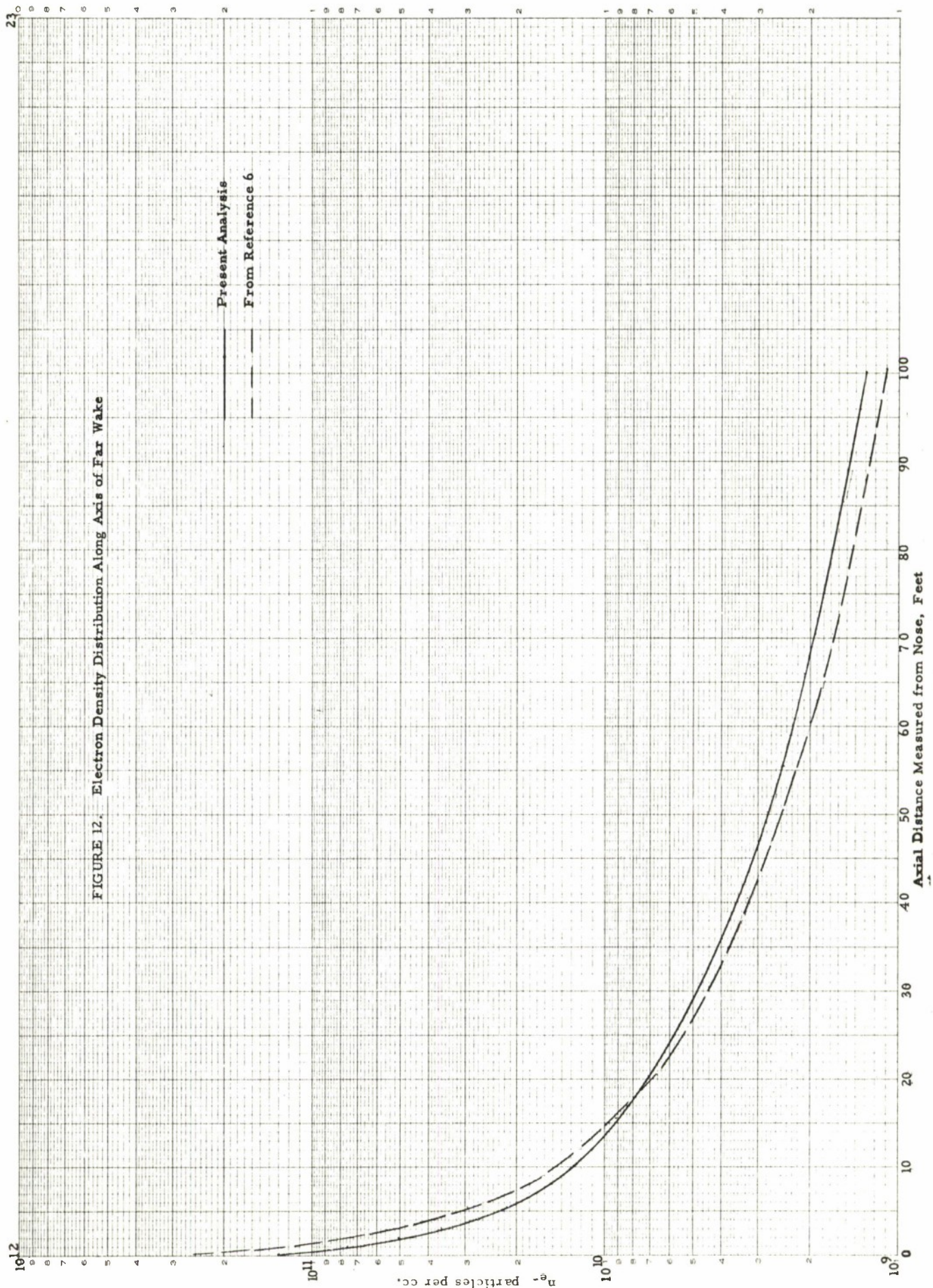


Figure 13. Temperature Distribution Along Axis of Far Wake

Present Analysis
From Reference 6

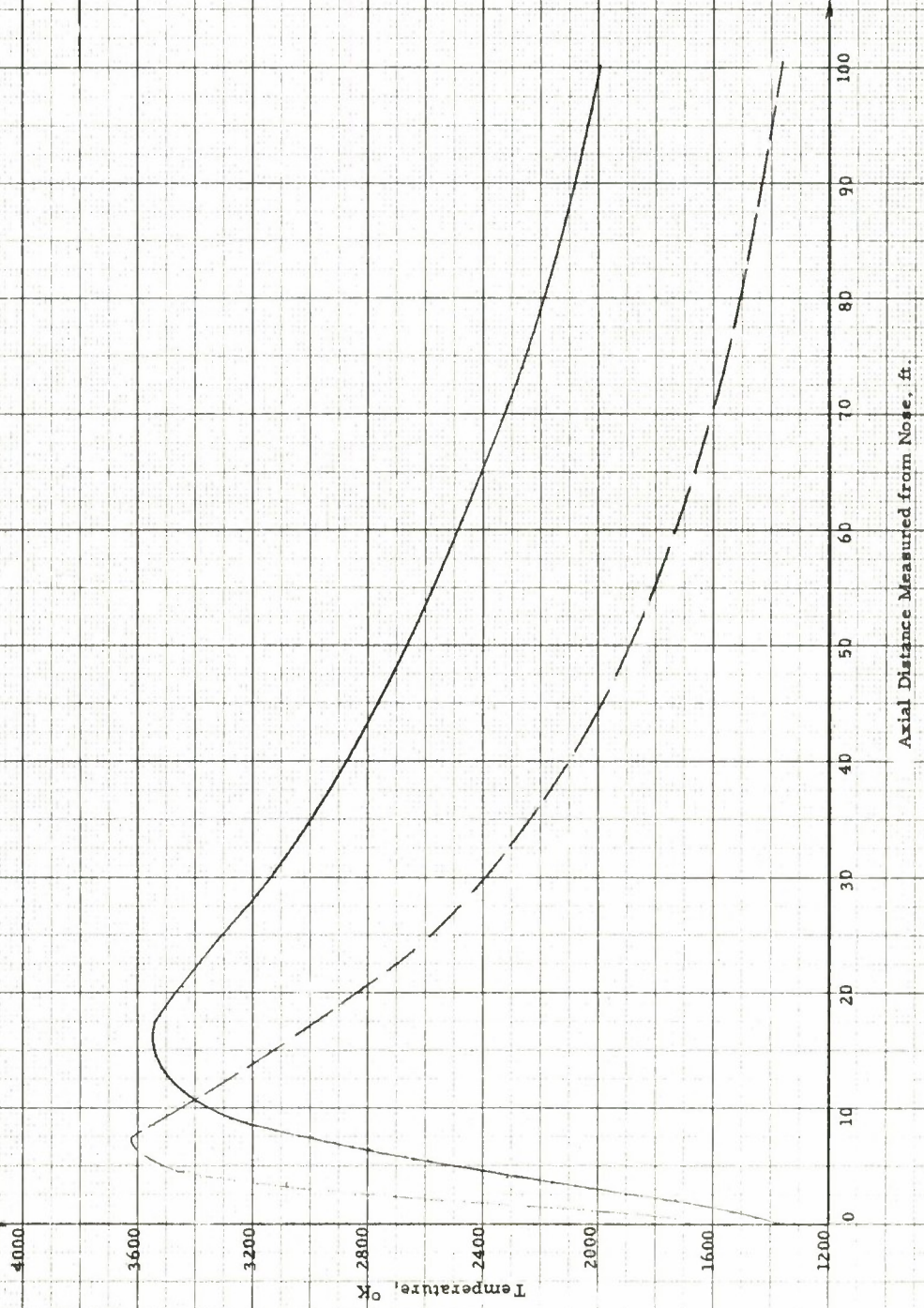
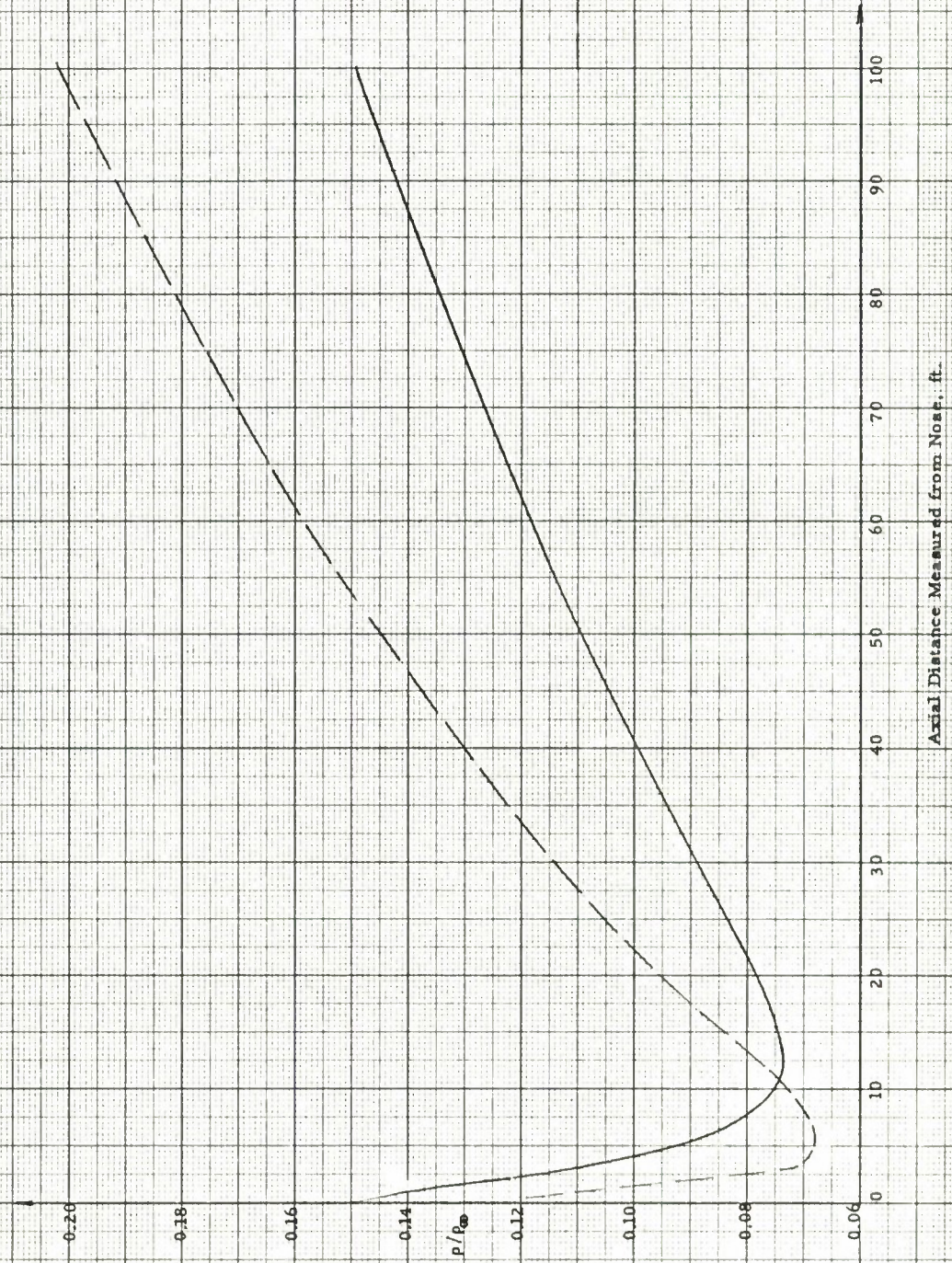


Figure 14. Density Distribution Along Axis of Far Wake



Present Analysis

From Reference 6

Axial Distance Measured from Nose, ft.

Figure 15. Velocity Distribution Along Axis of Far Wake

Present Analysis
From Reference 6

